

Induction of photoluminescence and columnar mesomorphism in hemi-disc salphen type Schiff bases via nickel(II) coordination

Chira R. Bhattacharjee*, Chitrani Datta, Gobinda Das, Rupam Chakrabarty, Paritosh Mondal

Department of Chemistry, Assam University, Silchar 788011, Assam, India

ARTICLE INFO

Article history:

Received 31 October 2011

Accepted 2 December 2011

Available online 13 December 2011

Keywords:

Nickel

Metallomesogen

Columnar mesomorphism

Density functional theory

ABSTRACT

A series of hemi-disc shaped non-mesomorphic tetradentate salicylaldehyde ligands [*N,N'*-di-(4-hexadecyloxysalicylidene)-1,2-diamino-benzene, *N,N'*-di-(4-hexadecyloxysalicylidene)-4-Me-1,2-diamino-benzene, and *N,N'*-di-(4-hexadecyloxysalicylidene)-4-NO₂-1,2-diamino-benzene, (H₂L)] were synthesized. Incorporation of nickel(II) in the tetradentate core via reaction with Ni(OAc)₂·4H₂O afforded a series of four coordinate mesogenic NiL derivatives. The ligands and complexes were characterized by elemental analyses, FT-IR, UV-Vis, FAB-mass, ¹H and ¹³C NMR (for ligands only). The mesomorphic behavior of the complexes were probed by polarizing optical microscopy, differential scanning calorimetry and powder X-ray diffraction technique. The non-mesogenic ligands upon coordination with nickel(II) exhibited monotropic/enantiotropic phase transition showing rectangular columnar mesophases (Col_r) with *c2mm* symmetry. A antiparallel dimeric association forming a disc-like arrangement in the mesophase is proposed on the basis of XRD-study. Solution electrical conductivity measurements are consistent with the non-electrolytic nature of the complexes. At room temperature with 330 nm excitation, the complexes showed blue emission both in the solid state (~481 nm, $\Phi = 7\%$) and in solution (~456 nm, $\Phi = 23\%$) while the ligands are non-emissive. The DFT study carried out at BLYP/DNP level revealed a distorted square planar structure for the nickel(II) complexes.

© 2011 Elsevier Ltd. All rights reserved.

1. Introduction

The technologies based on physical properties such as light emission or charge transport ability and related materials are currently receiving significant attention owing to their potential applications such as displays, solar cells, active components for image and data treatment storage etc. [1–5]. Of specific interest are luminescent liquid-crystalline materials that are considered very attractive for potential applications in optoelectronic devices because of their excellent charge-transport properties [1,3–10]. Combining luminescence properties in soft materials to generate new electronic devices is a fast growing field of research [3–10]. Design and synthesis of such luminescent photoresponsive liquid crystals is significant particularly in the context of their potential applications in organic light emitting diodes (OLEDs), information storage, sensors, and enhanced contrast displays [11,12]. Metallomesogens (metal containing liquid crystals) are ideal candidates for tuning smart multifunctional properties owing to the combination of optical, electronic and magnetic characteristics. Studies on light-emitting mesogens were mainly focused on organic compounds, while luminescent metallomesogens caught the fancy of researchers rather recently. Emissive metallomesogen with metals such as

lanthanides, Zn, Pd, Pt, Au, and Ag have been well documented [6–10]. We recently developed a series of photoluminescent metallomesogen based on salicylaldehyde Schiff-base ligands [11,13–15]. Transition metal complexes with salen-type ligands have been extensively studied mainly due to their ability to catalyze an extremely broad range of chemical transformations, including the asymmetric ring-opening of epoxides, aziridination, cyclopropanation, epoxidation of olefins and formation of cyclic and linear polycarbonates [16–19]. Moreover, nonlinear optical (NLO) properties of such materials have also been explored in recent years [20–23]. Nevertheless, application studies on metal–salen derivatives remained sparse in the literature, even though these compounds are known to be photoluminescent for a long time [20–25]. Choice of metal ion, nature and position of the substituents on side aromatic ring as well as spacers are known to greatly tune the mesogenic as well as photophysical behavior. For some compounds even a minor changes within the spacer can lead to major differences in molecular organization and in turn liquid-crystalline behavior [26–31]. Metal–salen complexes with 5-substituted alkoxy or alkyl chains exhibiting smectic mesomorphism are well documented [32–35]. Metallomesogen based on 4-substituted salen-type framework Schiff base ligands has been sparsely investigated [26–30]. Recently we have reported a series of structurally analogous 4-substituted zinc(II), oxovanadium(IV), Ni(II) as well as some copper(II) complexes, using cyclohexane/phenylene diamine spacer exhibited different type of columnar phase

* Corresponding author. Tel.: +91 03842 270848; fax: +91 03842 270342.

E-mail address: crbhattacharjee@rediffmail.com (C.R. Bhattacharjee).

[11,13,15,36–38]. Complexes with shorter alkoxy substituent, [VO(4-C_nH_{2n+1}O)₂Salen]ClO₄ (*n* = 3, 8, 10) with similar spacer lacked liquid crystalline behavior [26]. When complexed with non-discoid ligands, a molecular shape with a reduced length-to-breadth ratio is formed favouring a disc-like metallomesogens [39]. Such structures tend to form columnar mesophases [39]. Compounds exhibiting columnar phases with axially linked discs are of particular interest as potential one-dimensional photoconductors, semiconductors, or organic light emitting diodes (OLED) and photovoltaic cells [40–50]. A series of analogous nickel(II) complexes with cyclohexane spacer showing columnar rectangular mesophase have been reported recently by us [15]. However, there appears to be no record of nickel(II) complexes with rigid aromatic spacer. As a part of our continued and systematic investigation directed towards soft materials, in this article we describe synthesis of newer tetradentate Schiff base ligands bearing aromatic spacer with different electron withdrawing/donating substituent, and induction of luminescence and columnar mesomorphism via formation of hemi-disc shaped nickel(II) complexes. The ligands are non-mesogenic devoid of any luminescence.

2. Experimental

2.1. Physical measurements

The C, H and N analyses were carried out using PE2400 elemental analyzer. The ¹H NMR spectra were recorded on Bruker DPX-400 MHz spectrometer in CDCl₃ (chemical shift in δ) solution with TMS as internal standard. ¹³C NMR spectra were recorded on a JEOL AL300 FT NMR spectrometer. Molar conductance of the compounds was determined in CH₂Cl₂ (ca. 10⁻³ mol L⁻¹) at room temperature using MAC-554 conductometer. UV–Vis absorption spectra of the compounds in CH₂Cl₂ were recorded on a Shimadzu UV-160PC spectrophotometer. Photoluminescence spectra were recorded on a Shimadzu RF-5301PC spectrophotometer. The fluorescence quantum yield in dichloromethane was determined by dilution method using 9,10-diphenyl anthracene as standard. Infrared spectra were recorded on a Perkin–Elmer L 120-000A spectrometer on KBr disc. Mass spectra were recorded on a Jeol SX-102 spectrometer with fast atom bombardment. The optical textures of the different phase of the compounds were studied using a polarizing microscope (Nikon optiphot-2-pol) attached with Instec hot and cold stage HCS302, with STC200 temperature controller of 0.1 °C accuracy. The thermal behavior of the compounds were studied using a Perkin–Elmer differential scanning calorimeter (DSC) Pyris-1 spectrometer with a heating or cooling rate of 5 °C/min. Variable temperature powder X-ray diffraction (PXRD) of the samples were recorded on a Bruker D8 Discover instrument using CuKα radiation.

2.2. Computational analysis

All the structures were completely optimized using the hybrid HF-DFT method, labeled as BLYP. The BLYP functional is comprised of a hybrid exchange functional as defined by Becke and the non-local Lee–Yang–Parr correlation functional [51]. We used DFT semicore pseudopotential with double numerical basis set plus polarization functions (DNP), which is comparable with the Gaussian 6-31G(d,p) basis set in size and quality [52]. All structures were relaxed without any symmetry constraints. Convergence in energy, force, and displacement was set as 10⁻⁵ Hartree (Ha), 0.001 Ha/Å, and 0.005 Å, respectively. All calculations were performed with the DMol3 program package [52–54].

Global hardness (η) of an electronic system is defined [55] as the second derivative of total energy (E) with respect to the number of electrons (N) at constant external potential, $v(\vec{r})$

$$\eta = \frac{1}{2} \left(\frac{\delta^2 E}{\delta N^2} \right)_{v(\vec{r})} = \left(\frac{\delta \mu}{\delta N} \right)_{v(\vec{r})}$$

Global softness is the inverse of global hardness with a factor of half

$$S = \frac{1}{2\eta} = \left(\frac{\delta^2 N}{\delta E^2} \right)_{v(\vec{r})} = \left(\frac{\delta N}{\delta \mu} \right)_{v(\vec{r})}$$

By applying finite difference approximation the global hardness and softness are expressed as:

$$\eta = \frac{IE - EA}{2}, \quad S = \frac{1}{IE - EA}$$

where IE and EA are the first vertical ionization energy and the electron affinity of the molecule, respectively. Using Koopmans' theorem IE and EA can be approximated as negative of E_{HOMO} and E_{LUMO} , respectively and thus chemical hardness and chemical softness can be written as [56].

$$\eta = \frac{E_{\text{LUMO}} - E_{\text{HOMO}}}{2} \quad \text{and} \quad S = \frac{2}{E_{\text{LUMO}} - E_{\text{HOMO}}}, \quad \text{respectively.}$$

2.3. Materials

The materials were procured from Tokyo Kasei and Lancaster Chemicals. All solvents were purified and dried using standard procedures. Silica (60–120 mesh) from Spectrochem was used for chromatographic separation. Silica gel G (E-Merck, India) was used for TLC.

2.4. Synthesis of hexadecyloxysalicylaldehyde

Alkoxyaldehyde derivatives were prepared following reported method [11,13,15,36–38]. 2,4-Dihydroxybenzaldehyde (10 cm³, 1.38 g), KHCO₃ (10 cm³, 1.00 g), KI (catalytic amount) and 1-bromohexadecane (10 cm³, 2.8 g) were mixed in 250 mL of dry acetone. The mixture was heated under reflux for 24 h, and then filtered, while hot, to remove any insoluble solids. Dilute HCl was added to neutralize the warm solution followed by extraction with chloroform (100 cm³). The combined chloroform extract was concentrated to give a purple solid. The solid was purified by column chromatography using a mixture of chloroform and hexane (v/v , 1/1) as eluent. Evaporation of the solvents afforded a white solid product.

Synthesis of 16-opd and 16-mpd are reported in our earlier observations [11,13].

2.4.1. Synthesis of *N,N'*-bis(4-(4'-hexadecyloxy)-salicylidene)-4-NO₂-1,2-phenylenediamine (16-mpd)

An ethanolic solution of 2-hydroxy-(4-hexadecyloxy)-salicylaldehyde (0.39 g, 1 mmol) was added to an ethanolic solution of 4-NO₂-1,2-phenylenediamine (0.07 g, 0.5 mmol). The solution mixture was refluxed with a few drops of acetic acid as catalyst for 3 h to yield the yellow Schiff base *N,N'*-bis(4-(4'-*n*-alkoxy)-salicylidene)-4-NO₂-1,2-phenylenediamine. The compound was collected by filtration and recrystallized from absolute ethanol to obtain a pure compound.

Yield: 0.33 g, 75%. FAB Mass (m/e , fragment): m/z : calc. 841.6; found: 842.6 [M+H⁺]; Anal. Calc. for C₅₂H₇₉N₃O₆: C, 74.1; H, 9.4; N, 4.9. Found: C, 74.2; H, 9.5; N, 4.8%. ¹H NMR (400 MHz, CDCl₃): δ = 13.02 (s, 1H, H⁵), 8.78 (s, 1H, H⁴), 7.79 (d, J = 8.4 Hz, H⁹), 7.25 (d, 2H, H⁶), 7.18 (t, J = 8.2 Hz, 2H, H¹), 6.69 (d, J = 2.5 Hz, 2H, H³), 6.97 (dd, J = 2.4 Hz, J = 8.3 Hz, 2H, H²), 3.98 (t, J = 6.6 Hz, 2H, -OCH₂), 0.96 (t, J = 6.7 Hz, 6H, CH₃), 0.98 (m, -CH₂ of methylene pro-

ton in side chain); IR (ν_{\max} , cm^{-1} , KBr): 3513 (ν_{OH}), 2922 ($\nu_{\text{as}}(\text{C-H})$, CH_3), 2873 ($\nu_{\text{s}}(\text{C-H})$, CH_3), 1625 ($\nu_{\text{C=N}}$), 1294 ($\nu_{\text{C-O}}$).

2.4.2. Synthesis of nickel(II) complexes

General procedure. The ligand 16-opd (0.79 g, 1 mmol) or 16-mpd (0.81 g, 1 mmol) or 16-npd (0.84 g, 1 mmol) was dissolved in minimum volume of absolute ethanol. To this, an equimolar amount of nickel acetate $\text{Ni}(\text{OAc})_2 \cdot 4\text{H}_2\text{O}$ (0.02 g, 0.1 mmol) in methanol was then added slowly and stirred for 2 h at room temperature. A red solid formed immediately was filtered, washed with diethyl ether and recrystallized from chloroform–ethanol (1:1).

Ni-16opd. Yield = 0.60 g (75%). FAB Mass (m/e , fragment): m/z : calc. 852.5; found: 853.5 [$\text{M}+\text{H}^+$]; Anal. Calc. for $\text{C}_{52}\text{H}_{78}\text{N}_2\text{O}_4\text{Ni}$: C, 73.1; H, 9.2; N, 3.2. Found: C, 73.1; H, 9.2; N, 3.1%. ^1H NMR (400 MHz, CDCl_3): δ = 8.22 (s, 1H, H^4), 7.69 (d, J = 8.5 Hz, H^9), 7.17 (d, 2H, H^6), 7.10 (t, J = 8.4 Hz, 2H, H^1), 7.16 (dd, J = 2.3 Hz, J = 9.1, 2H, H^8), 6.61 (d, J = 2.4 Hz, 2H, H^3), 6.49 (dd, J = 2.4 Hz, J = 8.2 Hz, 2H, H^2), 3.95 (t, J = 6.8 Hz, 2H, $-\text{OCH}_2$), 0.91 (t, J = 6.8 Hz, 6H, CH_3), 0.87 (m, $-\text{CH}_2$ of methylene proton in side chain); IR (ν_{\max} , cm^{-1} , KBr): 2922 ($\nu_{\text{as}}(\text{C-H})$, CH_3), 2870 ($\nu_{\text{s}}(\text{C-H})$, CH_3), 1611 ($\nu_{\text{C=N}}$), 534 ($\nu_{\text{Ni-N}}$), 459 ($\nu_{\text{Ni-O}}$).

Ni-16mpd. Yield = 0.22 g, 76%. FAB Mass (m/e , fragment): m/z : calc. 866.5; found: 867.5 [$\text{M}+\text{H}^+$]; Anal. Calc. for $\text{C}_{53}\text{H}_{80}\text{N}_2\text{O}_4\text{Ni}$: C, 73.3; H, 9.2; N, 3.2. Found: C, 73.4; H, 9.3; N, 3.1%. ^1H NMR (400 MHz, CDCl_3): δ = 8.19 (s, 1H, H^4), 7.72 (d, J = 8.5 Hz, H^9), 7.21 (d, 2H, H^6), 7.11 (t, J = 8.4 Hz, 2H, H^1), 7.16 (dd, J = 2.33 Hz, J = 9.1, 2H, H^8), 6.61 (d, J = 2.4 Hz, 2H, H^3), 6.49 (dd, J = 2.44 Hz, J = 8.28 Hz, 2H, H^2), 3.92 (t, J = 6.8 Hz, 2H, $-\text{OCH}_2$), 0.91 (t, J = 6.8 Hz, 6H, CH_3), 0.87 (m, $-\text{CH}_2$ of methylene proton in side chain); IR (ν_{\max} , cm^{-1} , KBr): 2922 ($\nu_{\text{as}}(\text{C-H})$, CH_3), 2870 ($\nu_{\text{s}}(\text{C-H})$, CH_3), 1613 ($\nu_{\text{C=N}}$), 532 ($\nu_{\text{Ni-N}}$), 461 ($\nu_{\text{Ni-O}}$).

Ni-16npd. Yield = 0.64 g, 75%. FAB Mass (m/e , fragment): m/z : calc. 897.5; found: 898.5 [$\text{M}+\text{H}^+$]; Anal. Calc. for $\text{C}_{52}\text{H}_{77}\text{N}_3\text{O}_6\text{Ni}$: C, 69.4; H, 8.6; N, 4.6. Found: C, 69.3; H, 8.5; N, 4.5%. ^1H NMR (400 MHz, CDCl_3): δ = 8.23 (s, 1H, H^4), 7.77 (d, J = 8.5 Hz, H^9), 7.25 (d, 2H, H^6), 7.17 (t, J = 8.4 Hz, 2H, H^1), 7.18 (dd, J = 2.33 Hz, J = 9.1, 2H, H^8), 6.64 (d, J = 2.45 Hz, 2H, H^3), 6.42 (dd, J = 2.4 Hz, J = 8.2 Hz, 2H, H^2), 3.93 (t, J = 6.5 Hz, 2H, $-\text{OCH}_2$), 0.90 (t, J = 6.8 Hz, 6H, CH_3), 0.88 (m, $-\text{CH}_2$ of methylene proton in side chain); IR (ν_{\max} , cm^{-1} , KBr): 2921 ($\nu_{\text{as}}(\text{C-H})$, CH_3), 2870 ($\nu_{\text{s}}(\text{C-H})$, CH_3), 1616 ($\nu_{\text{C=N}}$), 531 ($\nu_{\text{Ni-N}}$), 457 ($\nu_{\text{Ni-O}}$).

3. Results and discussion

3.1. Synthesis and structural assessment

The compounds (16-opd/16-mpd/16-npd and Ni-16opd/Ni-16mpd/Ni-16npd) could be achieved through a facile and straightforward procedure [11,13,15,36–38]. The synthetic strategy for the ligands [$\text{L} = N,N$ -bis(4-(4'- n -hexadecyloxy)-salicylidene)1,2-phenylenediamine/4-Me-1,2-phenylenediamine/4- NO_2 -1,2-phenylenediamine), hereafter abbreviated as 16-opd/16-mpd/16-npd] and the Ni(II) complexes (Ni-16opd/Ni-16mpd/Ni-16npd) are presented in Scheme 1. The complexes (Ni-16opd/Ni-16mpd/Ni-16npd), were prepared by the reaction of appropriate ligand with nickel acetate (1:1 molar ratio) in ethanol/methanol and recrystallized from methanol/ CH_2Cl_2 ; the complexes were isolated as red colored solids in good yields. The compounds were characterized by ^1H and ^{13}C NMR, FT-IR, UV-Vis spectroscopy and elemental analysis. From the IR study, it was found that the shift of ν_{CN} vibrational stretching frequency at ca.1625 cm^{-1} to lower wave number ($\Delta\nu \sim 30 \text{ cm}^{-1}$) and absence of ν_{OH} mode upon chelation, clearly suggested the coordination of azomethine-N and phenolate-O to the metal. Appearance of additional bands at ~ 450 – 480 and ~ 527 – 549 cm^{-1} in the

spectra of the complexes assigned to Ni–O and Ni–N stretching vibrations that are not observed in the spectra of the ligands furnished evidence for [N,O] binding mode of the ligand. The $\nu_{\text{C=N}}$ stretching frequency is rather independent of the length of alkoxy side chain in both ligands and their complexes. The FAB-mass spectra of the compounds matched well with their formula weights. Solution electrical conductivity of complexes recorded in CH_2Cl_2 (10^{-3} M) was found to be $<10 \Omega^{-1} \text{ cm}^{-1} \text{ mol}^{-1}$, much lower than is expected for a 1:1 electrolyte, thus confirming the non-electrolytic nature of the complex. ^1H NMR spectra of the ligands showed two characteristic signals at $\delta = 13.4$ – 13.8 ppm corresponding to the OH proton and at $\delta = 8.5 \text{ ppm}$ due to the imine proton. Moreover upon complexation, lack of proton signal corresponding to the OH group of the free ligands and the upfield shift of the imine proton further attested the coordination of azomethine-N.

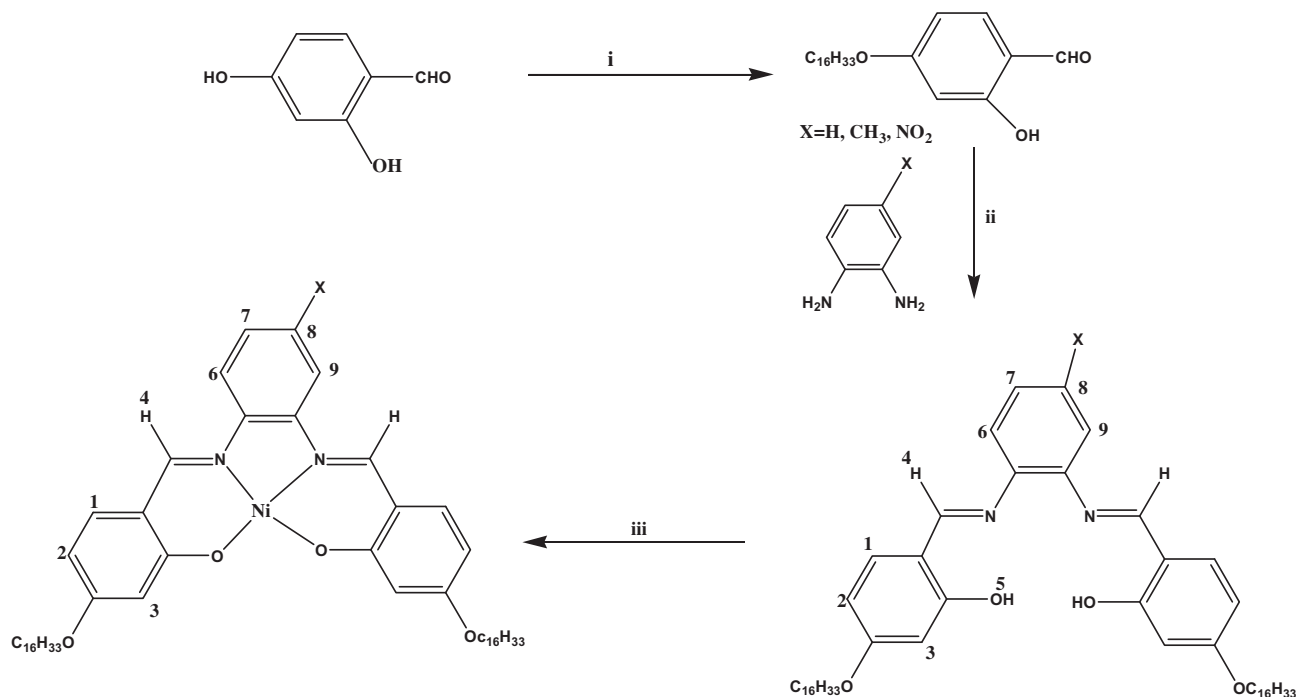
3.2. Photophysical properties

The electronic spectra of the free ligands exhibited three bands (Fig. 1) in the region of ~ 288 – 366 nm assigned to π – π^* transitions, which involves molecular orbitals essentially localized on the C=N group and the benzene ring. The absorption maxima are red shifted in 16-npd ligand owing to the presence of the NO_2 chromophore in the ligand. The complexes exhibited two intense red shifted bands (Fig. 2) at ~ 312 – 325 nm and ~ 383 – 401 nm resulting from the metal-perturbed ligand-centered transitions, which have the same origin as the two principal bands of the ligand spectrum. In addition, the complexes also displayed a broad unstructured low intensity band centered at ~ 447 – 462 nm assigned to ligand to metal charge transfer transitions (LMCT) charge transfer transition ($\text{N} \rightarrow \text{Ni}^{2+}$) which might have obscured the d–d bands.

The photoluminescence properties of the compounds were investigated in dichloromethane solution and in thin films, at room temperature. The ligands are non-emissive, but their corresponding Ni(II) complexes displayed strong blue emission both in solution and solid state (Fig. 3), usually observed in similar Schiff-based metal complexes, with the emission maximum centered at ~ 454 – 488 nm originating from π – π^* singlet ligand-centered excited state [57–60,32]. The emission maxima for typical compound Ni-18opd in solid state ($\sim 481 \text{ nm}$, $\Phi = 7\%$) is considerably red shifted with respect to that recorded in solution ($\sim 456 \text{ nm}$, $\Phi = 23\%$). In solid state after complexation, the free rotation of the flexible bonds of the ligand is reduced and hence energy dissipation through non-radiative channels decreases leading to shift of emission wavelength to lower energy. Moreover in the solid state, a larger electronic delocalization and intermolecular aromatic interaction leads to a lowering of energy of the electronic states [57–60,32]. The spectral data are summarized in Table 1.

3.3. Thermal microscopy and differential scanning calorimetry study

The thermal behavior of the compounds (Table 2) was investigated by polarizing optical microscopy (POM) and differential scanning calorimetry (DSC) study. The ligands are found to be non-mesomorphic. However, on co-ordination to nickel(II) ion mesomorphism was induced, reflecting conformational rigidification of the ligand on complexation. Monotropic mesomorphism was encountered for Ni-16npd and Ni-16mpd complexes. The Ni-16opd showed enantiotropic mesomorphic behavior. Polarized optical microscopy of a representative complex (Ni-16opd) revealed that, upon cooling the sample from isotropic phase, a spherulitic growth appeared which coalesce to a fan-like texture (Fig. 4) at $\sim 130 \text{ }^\circ\text{C}$ with large homeotropic regions, suggesting a columnar mesophase (Col). The mesophase is stable down to room temperature. The DSC thermogram (Fig. 5) for the complex (Ni-16opd) exhibited two transitions in heating and two in cooling cycle.



Scheme 1. (i) $C_{16}H_{33}Br$, $KHCO_3$, KI , dry acetone, Δ , 40 h, (ii) glacial AcOH, absolute EtOH, Δ , 4 h and (iii) $Ni(OAc)_2 \cdot 4H_2O$, MeOH, Stirr, 2 h.

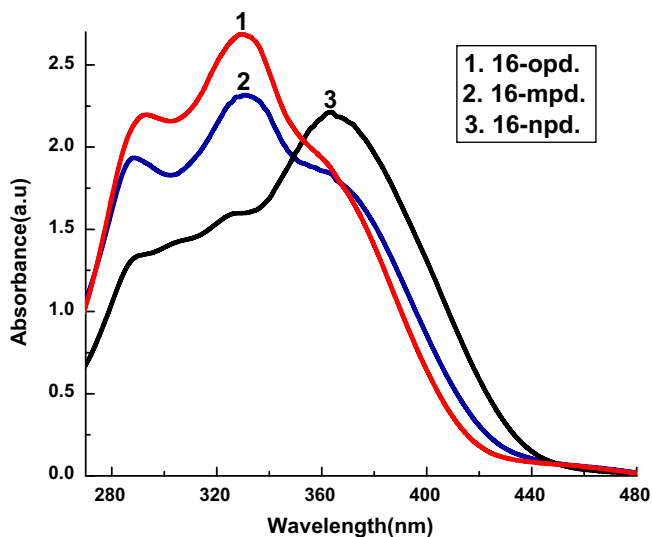


Fig. 1. Absorption spectra of the ligands.

The melting temperatures of the complexes showed a decreasing trend with $X = H, CH_3,$ and NO_2 in that order (Table 2). The isotropisation temperatures, however, reflected a different trend with the nitro substituted complex exhibiting highest value (209.2 °C) and the methyl substituted one showing the least (125.2 °C). Another interesting aspect is the quite low enthalpy values for the phase transitions in the unsubstituted complex (Ni-16opd) compared to those observed for the substituted ones (Ni-16mpd and Ni-16npd). In general, complexes with higher molecular weights tend to exhibit larger enthalpy changes during mesophase to isotropic liquid transitions [27]. Relatively high enthalpies for mesophase transition to isotropic state in the substituted complexes, Ni-16mpd and Ni-16npd could be indicative of the formation of a higher order columnar phase in this system [61].

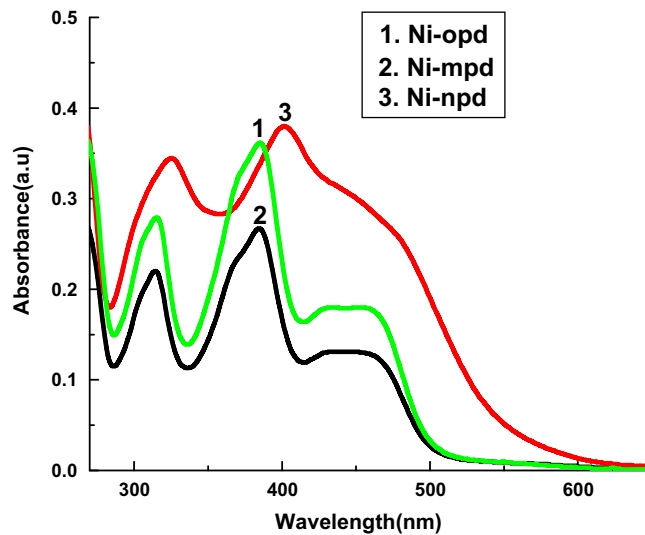


Fig. 2. Absorption spectra of the complexes.

In our earlier reports, we have found that, the VO-16opd showed lamellar columnar mesomorphism (Col_l) [36]. However, Zn-16opd/Zn-16mpd complexes exhibited columnar rectangular (Col_r/Col_h) mesophase [11,13].

3.4. XRD-study

The mesophase structure was confirmed by temperature-dependent X-ray diffraction analysis (Table 3). The spectrum was recorded for a typical compound, Ni-16opd at 130 °C. In the low angle region two fundamental sharp reflections were observed characteristic of a rectangular columnar mesophase (Fig. 6). Further, there are two diffuse reflections in the wide angle region. One corresponds to 4.9 Å, for molten alkyl chains, the

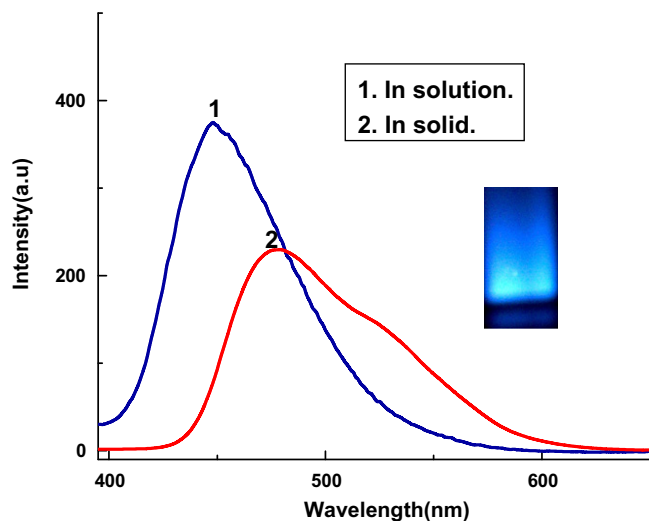


Fig. 3. Emission spectra of the Ni-16opd complex.

Table 1
UV–Vis and photoluminescence data of the compounds.

Compounds	$\pi \rightarrow \pi^*$ (ϵ , l mol ⁻¹ cm ⁻¹)	LMCT (ϵ , l mol ⁻¹ cm ⁻¹)	PL ^a (solution)	PL ^a (solid)
16opd	292 nm (22000) 329 nm (26800) 363 nm (18981)			
Ni-16opd	315 nm (2770) 385 nm (3610)	447 nm (1800)	456 nm	481 nm
16mpd	289 nm (19300) 330 nm (23100) 365 nm (18110)			
Ni-16mpd	314 nm (2200) 385 nm (2670)	448 nm (1310)	454 nm	478 nm
16npd	295 nm (13400) 335 nm (16851) 367 nm (21850)			
Ni-16npd	326 nm (3450) 402 nm (3800)	462 nm (2820)	468 nm	488 nm

^a Photoluminescence data.

relatively sharper one at about 3.6 Å, well separated from the broad peak is due to the regular stacking of the molecules within the columnar mesophase. In the wide angle region the presence of another less broad peak at about 7.6 Å may indicate the formation of dimers (Fig. 7) along the axis of the column. Moreover, due to the absence of (21) peak in the XRD spectrum, the symmetry of the lattice can be further assigned to a *c2mm* plane group [39,62,63]. The lattice constants of this rectangular phase are $a = 38.2$ Å and $b = 15.4$ Å. The lattice parameter $a = 38.2$ Å is larger than the radius of the half-disc shaped molecule (~ 20.6 Å). Therefore the hemi-disc molecules in the mesophase are believed to organize themselves in an anti-parallel fashion (Fig. 7). A similar type of molecular self assembly was reported earlier [15,37,39,64].

3.5. DFT-study

The optimized structure of the complex is shown in (Fig. 8). The complexes are neutral with Ni²⁺ in d⁸-system. We optimized singlet and triplet state of the complexes and found singlet square planar geometry is more stable. The 3D isosurface plots of the lowest unoccupied molecular orbital (LUMO) and the

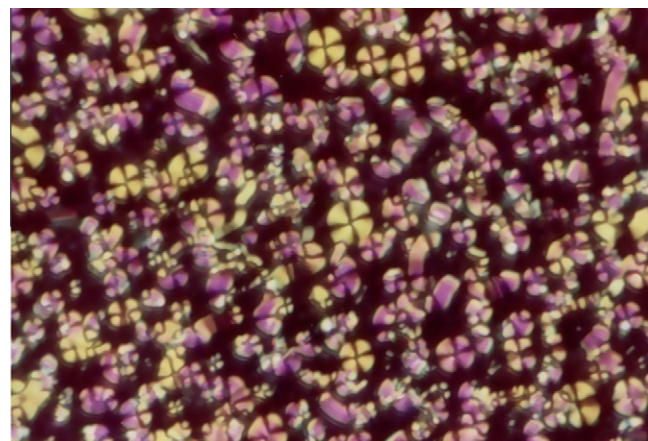


Fig. 4. POM texture of Ni-16opd complex.

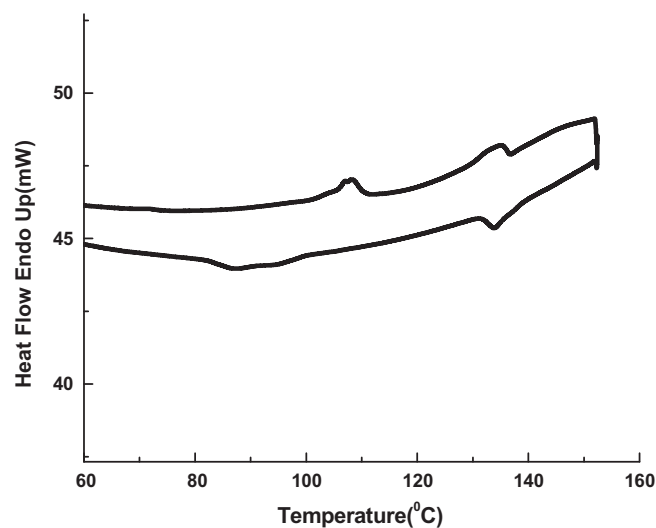


Fig. 5. DSC thermogram of Ni-16opd complex.

Table 2
POM and DSC data of the complexes.

Compounds	T (°C)	Transition	ΔH (kJ mol ⁻¹)
Ni-16opd	108.2 (heating)	Cr–Col _r	2.9
	135.0 (heating)	Col _r –I	2.6
	133.9 (cooling)	I–Col _r	2.5
Ni-16mpd	87.1 (cooling)	Col _r –Cr	0.93
	84.4 (heating)	Cr–Col _r	12.8
Ni-16npd	125.2 (heating)	Col _r –I	12.9
	78.3 (heating)	Cr–Col _r	14.8
	209.2 (heating)	Col _r –I	15.4

highest occupied molecular orbital (HOMO) for the nickel complex (Ni-16opd) is shown in (Figs. 9 and 10). In all the complexes, electron density of the HOMO is mainly localized in between Ni–O and Ni–N bonds, while the electron density of the LUMO is localized on nickel atoms. The Ni–O (apical) interaction in the dimer (Figs. 9 and 10) expectedly occur between molecular orbitals of sigma (O) and pi*(Ni). The HOMO, LUMO energy difference of the complexes depends on the electronic nature of the substituents [65–67]. The energy differences decrease in the order of Ni-16mpd > Ni-16opd > Ni-16npd. The HOMO–LUMO energy separation can be used as a measure of

Table 3
XRD-data of the Ni-16opd.

Compound	$D_{\text{obs.}}$ (Å) ^a	$D_{\text{calc.}}$ (Å) ^b	hk^c	Parameters ^d
Ni-16opd	19.3	19.2	20	$\text{Col}_I - c2mm$
	14.1	14.3	11	$a = 38.2 \text{ \AA}$
	10.3	10.4	31	$b = 15.4 \text{ \AA}$
	7.6			$S = 588.3 \text{ \AA}^2$
	4.9			$V_m = 1551 \text{ \AA}^3$
	3.5			$h = 2.1 \text{ \AA}$
				$S_{\text{col}} = 294.1$

^a $D_{\text{obs.}}$ is experimentally and theoretically measured diffraction spacings at 130 °C.

^b $D_{\text{calc.}}$ is experimentally and theoretically measured diffraction spacings at 130 °C.

^c hk are indexation of the reflections.

^d Mesophase parameters, molecular volume V_m is calculated using the formula: $V_m = M/\lambda\rho N_A$, where M is the molecular weight of the compound, N_A is the Avogadro number, ρ is the volume mass ($\approx 1 \text{ g cm}^{-3}$), and $\lambda(T)$ is a temperature correction coefficient at the temperature of the experiment (T). $\lambda = \text{VCH}_2(T_0)/\text{VCH}_2(T)$, $T_0 = 25 \text{ }^\circ\text{C}$. $\text{VCH}_2(T) = 26.5616 + 0.02023(T)$. h is the intermolecular repeating distance deduced directly from the measured molecular volume and the lattice area according to $h = V_m/S$. For the Col_I phase, the lattice parameters a and b are deduced from the mathematical expression: $a = 2d_{20}$ and $1/d_{hk} = \sqrt{h^2/a^2 + k^2/b^2}$, where a , b are the parameters of the Col_I phase, S is the lattice area, S_{col} is the columnar cross-section ($S = ab$, $S_{\text{col}} = S/2$).

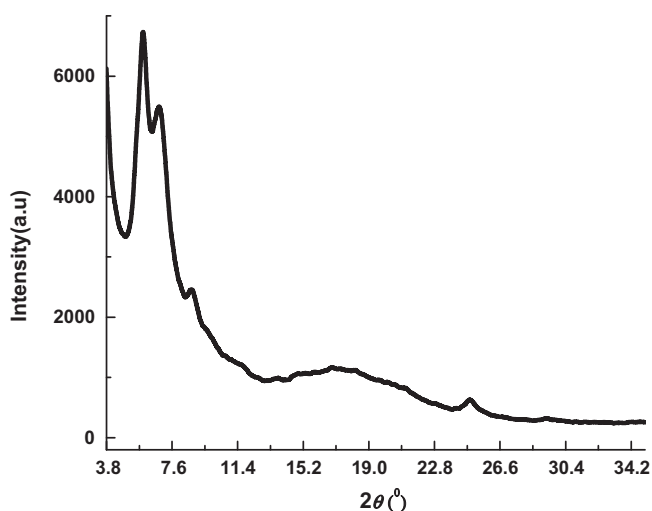


Fig. 6. XRD-pattern of Ni-16opd.

kinetic stability of the molecule and could indicate the reactivity pattern of the molecule. A small HOMO–LUMO gap implies a low kinetic stability and high chemical reactivity, because it is energetically favorable to add electrons to LUMO or to extract electrons from a HOMO. We further calculated the chemical softness values for both model complexes from their HOMO and LUMO energies. The chemical softness values of hydrogen, methyl and nitro-substituted complexes are 2.058, 2.051 and 3.643 eV^{-1} , respectively. The higher softness value obtained for the later complex indicated the lower stability of the complex compared to the hydrogen and methyl containing one. Some of the selective geometric parameters of optimized hydrogen, methyl and nitro-substituted nickel complex, evaluated by DFT calculation at BLYP/DNP level are reported in Table 4. From DFT data, it is noticed that the complexes have an average Ni–O and Ni–N bond lengths are in the range of 1.93–1.92 and 2.00–1.99 Å, respectively. The average bond angles are in the range of 94.70–92.8 and 83.20–83.6 for O1–Ni–O2 and N1–

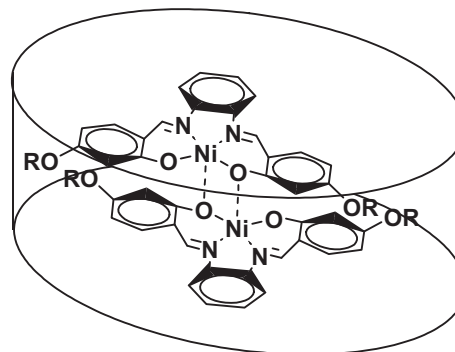


Fig. 7. Dimeric interaction of molecules.

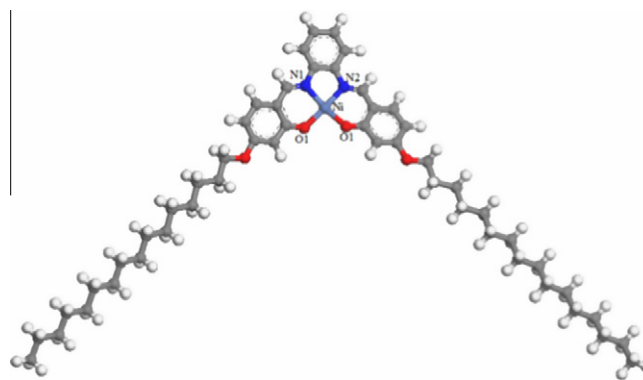


Fig. 8. Optimized structure of Ni-16opd.

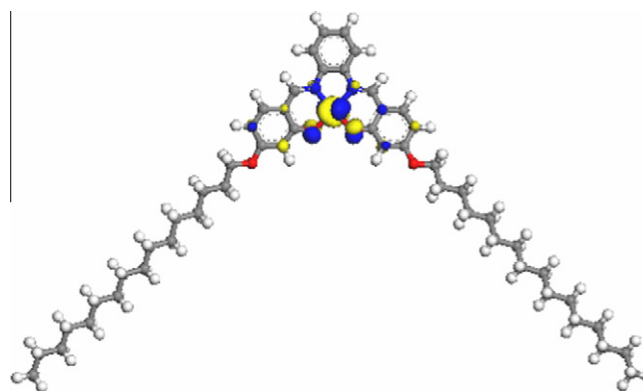


Fig. 9. LUMO energy diagram of Ni-16opd.

Ni–N2, respectively, around the nickel atom deviate substantially from the tetrahedral values indicating a distorted planar four coordinate geometry. The dihedral angles O(1)O(2)N(1)N(2) and N(1)O(1)O(2)N(2) as computed from DFT are found to lie in the range 15–20° (Table 4) reflecting the deviation from planarity. A strained conformation of the $[\text{N}_2\text{O}_2]$ -donor tetradentate ligand with long pendant alkyl side chains is believed to have caused the deviation from planar symmetry. Moreover, a short rigid central spacer group in the present complexes presumably prevented the formation of a tetrahedral environment around nickel(II), leading to a distorted square planar geometry. The length of the complexes based on the fully extended structure is found to be $\sim 40.7 \text{ \AA}$ (measured from the two terminal end of the side alkyl chain).

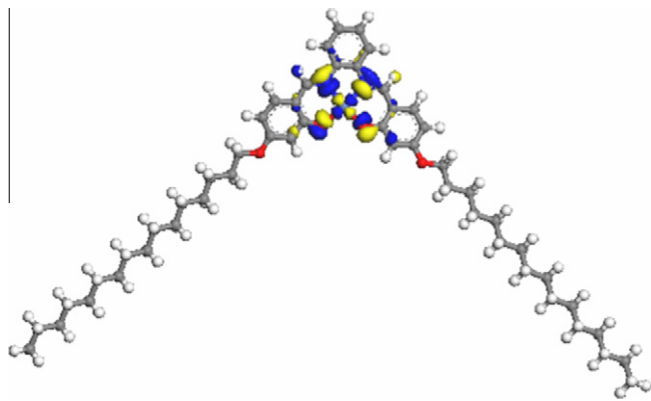


Fig. 10. HOMO energy diagram of Ni-16opd.

Table 4

DFT data of the complexes. Bond lengths are reported in Å and bond angles in degrees.

Structure parameter	Ni-opd	Ni-mpd	Ni-npd
Ni–O(1)	1.929	1.930	1.921
Ni–O(2)	1.930	1.931	1.919
Ni–N(1)	1.999	1.999	1.989
Ni–N(2)	1.999	2.001	1.983
O(1)–Ni–O(2)	94.67	94.58	92.84
N(1)–Ni–N(2)	83.16	83.20	83.56
N(1)–Ni–O(2)	165.14	165.65	167.55
O(1)–Ni–N(1)	92.76	92.71	92.72
O(1)–Ni–N(2)	165.29	165.45	167.98
N(2)–Ni–O(2)	92.63	92.58	93.09
HOMO in eV	–3.584	–3.542	–3.920
LUMO in eV	–2.612	–2.567	–3.371
ΔE in eV	0.972	0.975	0.549
Chemical softness	2.058	2.051	3.643
O(1)O(2)N(2)N(1)	19.3	18.8	16.2
N(1)O(1)O(2)N(2)	17.9	17.5	15.0

4. Conclusion

A new series of Ni(II)–salphen complexes bearing differently substituted aromatic spacer have been successfully synthesized. Lower conductivity values confirm the non electrolytic nature of the complexes. The ligands are found to be non-mesogenic and non-luminescent, however, all the complexes exhibited unprecedented columnar rectangular structure with $c2mm$ symmetry and also exhibited intense blue light emission both in solid state and solution. Based on the spectral and DFT study, a distorted square planar geometry around the Ni(II) center have been conjectured. The mesomorphic behavior of the complexes as a function of the spacer substituent is collated.

Acknowledgments

The authors thank SAIF, NEHU and CDRI, Lucknow for analytical and spectral data. CD acknowledges financial support from UGC, Government of India. Dr. R.C. Deka, Tezpur University, India, is acknowledged for computational facility.

References

- [1] Y. Molard, F. Dorson, V. Circu, T. Roisnel, F. Artzner, S. Cordier, *Angew. Chem., Int. Ed.* 49 (2010) 3351.
- [2] C.S. Pecinovsky, E.S. Hatakeyama, D.L. Gin, *Adv. Mater.* 20 (2008) 174.
- [3] X. Feng, W. Pisula, L. Zhi, M. Takase, K. Mullen, *Angew. Chem., Int. Ed.* 47 (2008) 1703.
- [4] M.J. Baena, P. Espinet, C.L. Folcia, J. Ortega, J. Etxebarria, *Inorg. Chem.* 49 (2010) 8904.
- [5] J. Arias, M. Bardaji, P. Espinet, C.L. Folcia, J. Ortega, J. Etxebarria, *Inorg. Chem.* 48 (2009) 6205.
- [6] E. Terazzi, S. Torelli, G. Bernardinelli, J.-P. Rivera, J.-M. Benech, C. Bourgogne, B. Donnio, D. Guillon, D. Imbert, J.-C.G. Bunzli, A. Pinto, D. Jeannerat, C. Piguet, *J. Am. Chem. Soc.* 127 (2005) 888.
- [7] M. Ghedini, D. Pucci, A. Crispini, A. Bellusci, M. La Deda, I. Aiello, T. Pugliese, *Inorg. Chem. Commun.* 10 (2007) 243.
- [8] F. Camerel, R. Ziessel, B. Donnio, C. Bourgogne, D. Guillon, M. Schmutz, C. Iacovita, J.-P. Bucher, *Angew. Chem., Int. Ed.* 46 (2007) 2659.
- [9] V.N. Kozhevnikov, B. Donnio, D.W. Bruce, *Angew. Chem., Int. Ed.* 47 (2008) 6286.
- [10] D. Pucci, G. Barberio, A. Bellusci, A. Crispini, M. La Deda, M. Ghedini, E.I. Szerb, *Eur. J. Inorg. Chem.* (2005) 2457.
- [11] C.R. Bhattacharjee, G. Das, P. Mondal, N.V.S. Rao, *Polyhedron* 29 (2010) 3089.
- [12] K. Binnemans, *J. Mater. Chem.* 19 (2009) 448.
- [13] C.R. Bhattacharjee, G. Das, P. Mondal, S.K. Prasad, D.S.S. Rao, *Eur. J. Inorg. Chem.* (2011) 1418.
- [14] C.R. Bhattacharjee, G. Das, P. Goswami, P. Mondal, S.K. Prasad, D.S.S. Rao, *Polyhedron* 30 (2011) 1040.
- [15] C.R. Bhattacharjee, G. Das, P. Mondal, *Eur. J. Inorg. Chem.* (2011) 5390.
- [16] P.G. Cozzi, L.S. Dolci, A. Garelli, M. Montalti, L. Prodi, N. Zaccheroni, *New J. Chem.* 27 (2003) 692.
- [17] P.G. Cozzi, *Chem. Soc. Rev.* 33 (2004) 410.
- [18] C. Gennari, U. Piarulli, *Chem. Rev.* 103 (2003) 3071.
- [19] R.I. Kureshy, I. Ahmad, N.H. Khan, S.H.R. Abdi, K. Pathak, *J. Catal.* 238 (2006) 134.
- [20] V. Aubert, V. Guerschais, E. Ishow, K.T. Hoang, I. Ledoux, K. Nakatani, L.H. Bozec, *Angew. Chem., Int. Ed.* 47 (2008) 577.
- [21] B.J. Coe, in: J.A. McCleverty, T.J. Meyer (Eds.), *Comprehensive Coordination Chemistry II*, vol. 9, Elsevier Pergamon, Oxford, 2004, pp. 621–687.
- [22] J. Chiffre, F. Averseng, G.G.A. Balavoine, J.-C. Daran, G. Iftime, P.G. Lacroix, E. Manoury, K. Nakatani, *Eur. J. Inorg. Chem.* (2001) 2221.
- [23] I. Sasaki, L. Vender, A.S. Saquet, P.G. Lacroix, *Eur. J. Inorg. Chem.* (2006) 3294.
- [24] I. Aiello, M. Ghedini, F. Neve, D. Pucci, *Chem. Mater.* 9 (1997) 2107.
- [25] A.K. Singh, S. Kumari, K.R. Kumar, B. Sridhar, T.R. Rao, *Polyhedron* 27 (2008) 181.
- [26] Y. Abe, A. Iyoda, K. Seto, A. Moriguchi, T. Tanase, H. Yokoyama, *Eur. J. Inorg. Chem.* (2008) 2148.
- [27] Y. Abe, K. Nakabayashi, N. Matsukawa, H. Takashima, M. Iida, T. Tanase, M. Sugibayashi, H. Mukai, K. Ohta, *Inorg. Chim. Acta* 359 (2006) 3934.
- [28] Y. Abe, N. Nakazima, T. Tanase, S. Katano, H. Mukai, K. Ohta, *Mol. Cryst. Liq. Cryst.* 466 (2007) 129.
- [29] Y. Abe, K. Nakabayashi, N. Matsukawa, M. Iida, T. Tanase, M. Sugibayashi, K. Ohta, *Inorg. Chem. Commun.* 7 (2004) 580.
- [30] Y. Abe, H. Akao, Y. Yoshida, H. Takashima, T. Tanase, H. Mukai, K. Ohta, *Inorg. Chim. Acta* 359 (2006) 3147.
- [31] A. Glebowska, P. Przybylski, M. Winek, P. Krzyczkowska, A. Krowczynski, Z. Szydłowska, D. Pocięcha, E. Gorecka, *J. Mater. Chem.* 19 (2009) 1395.
- [32] E. Caverio, S. Uriel, P. Romero, J.L. Serrano, R. Giménez, *J. Am. Chem. Soc.* 129 (2007) 11608.
- [33] Z. Rezvani, A.R. Abbasi, K. Nejati, M. Seyedahmadian, *Polyhedron* 24 (2005) 1461.
- [34] K. Nejati, Z. Rezvani, *New J. Chem.* 27 (2003) 1665.
- [35] Z. Rezvani, M.A. Ghanea, K. Nejati, S.A. Baghaei, *Polyhedron* 28 (2009) 2913.
- [36] C.R. Bhattacharjee, G. Das, P. Mondal, S.K. Prasad, D.S.S. Rao, *Inorg. Chem. Commun.* 14 (2011) 606.
- [37] C.R. Bhattacharjee, G. Das, P. Mondal, *Liq. Cryst.* 38 (2011) 441.
- [38] C.R. Bhattacharjee, G. Das, P. Mondal, S.K. Prasad, D.S.S. Rao, *Liq. Cryst.* 38 (2011) 615.
- [39] F. Morale, R.W. Date, D. Guillon, D.W. Bruce, R.L. Finn, C. Wilson, A.J. Blake, M. Schroder, B. Donnio, *Chem. Eur. J.* 9 (2003) 2484.
- [40] S. Kumar, *Chem. Soc. Rev.* 35 (2006) 83.
- [41] J.W. Goodby, V. Gortz, S.J. Cowling, G. Mackenzie, P. Martin, D. Plusquellec, T. Benvegnu, P. Boullanger, D. Lafont, Y. Queneau, S. Chambert, J. Fitremann, *Chem. Soc. Rev.* 36 (2007) 1971.
- [42] M. O'Neill, S.M. Kelly, *Adv. Mater.* 15 (2003) 1135.
- [43] R. Cristiano, H. Gallardo, A.J. Bortoluzzi, I.H. Bechtold, C.E.M. Campos, R.L. Longo, *Chem. Commun.* (2008) 5134.
- [44] S. Sergeyev, W. Pisula, Y.H. Geerts, *Chem. Soc. Rev.* 36 (2007) 1902.
- [45] Y. Shirota, H. Kageyama, *Chem. Rev.* 107 (2007) 953.
- [46] M. Sawamura, K. Kawai, Y. Matusuo, K. Kanie, T. Kato, *Nature* 419 (2002) 702.
- [47] I. Seguy, P. Jolinat, P. Destruel, R. Mamy, *J. Appl. Phys.* 89 (2001) 5442.
- [48] A.M. Van de Craats, N. Stutzmann, M.M. Nielsen, M. Watson, *Adv. Mater.* 15 (2003) 495.
- [49] S. Laschat, A. Baro, N. Steinke, F. Giesselmann, C. Hagele, G. Scalia, R. Judele, E. Kapatsina, S. Sauer, A. Schreivogel, M. Tosoni, *Angew. Chem., Int. Ed.* 46 (2007) 4832.
- [50] D. Pucci, I. Aiello, A. Bellusci, A. Crispini, M. Ghedini, M. La Deda, *Eur. J. Inorg. Chem.* (2009) 4274.
- [51] C. Lee, W. Yang, R.G. Parr, *Phys. Rev. B* 37 (1988) 785.
- [52] B. Delley, *J. Chem. Phys.* 92 (1990) 508.
- [53] B. Delley, *J. Chem. Phys.* 113 (2000) 7756.
- [54] B. Delley, *J. Phys. Chem.* 100 (1996) 6107.
- [55] R.G. Parr, R.G. Pearson, *J. Am. Chem. Soc.* 105 (1983) 7512.
- [56] T.A. Koopmans, *Physica* 1 (1933) 104.

- [57] Y.H. Xing, J. Han, G.H. Zhou, Z. Sun, X.J. Zhang, B.L. Zhang, Y.H. Zhang, H.Q. Yuan, M.F. Ge, *J. Coord. Chem.* 61 (2008) 715.
- [58] J.-M. Lin, W.-B. Chen, X.-M. Lin, A.-H. Lin, C.-Y. Ma, W. Dong, C.-E. Tian, *Chem. Commun.* 47 (2011) 2402.
- [59] T. Chattopadhyay, M. Mukherjee, K.S. Banu, A. Banerjee, E. Suresh, E. Zangrando, D. Das, *J. Coord. Chem.* 62 (2009) 967.
- [60] H.-J. Son, W.-S. Han, J.-Y. Chun, B.-K. Kang, S.-N. Kwon, J. Ko, S.J. Han, C. Lee, S.J. Klm, S.O. Kang, *Inorg. Chem.* 47 (2008) 5666.
- [61] D. Pucci, A. Crispini, M. Ghedini, E.I. Sezerb, M. La Deda, *Dalton Trans.* 40 (2011) 4614.
- [62] A.G. Serrette, C.K. Lai, T.M. Swager, *Chem. Mater.* 6 (1994) 2252.
- [63] H. Zheng, C.K. Lai, T.M. Swager, *Chem. Mater.* 7 (1995) 2067.
- [64] S.T. Trzaska, T.M. Swager, *Chem. Mater.* 10 (1998) 438.
- [65] Z. Zhou, R.G. Parr, *J. Am. Chem. Soc.* 112 (1990) 5720.
- [66] J.-I. Aihara, *J. Phys. Chem. A* 103 (1999) 7487.
- [67] Z. Zhou, R.G. Parr, *J. Am. Chem. Soc.* 111 (1989) 7371.